

HEAT TRANSFER ANALYSIS IN MULTI-CONFIGURATION MICROCHANNEL HEAT
SINK

IHSAN ALI GHANI

UNIVERSITI TEKNOLOGI MALAYSIA

HEAT TRANSFER ANALYSIS IN MULTI-CONFIGURATION
MICROCHANNEL HEAT SINK

IHSAN ALI GHANI

A thesis submitted in fulfilment of the
requirements for the award of the degree of
Doctor of Philosophy (Mechanical Engineering)

Faculty of Mechanical Engineering
Universiti Teknologi Malaysia

AUGUST 2017

To my supervisors, soul of my father, my mother and family for taking care
of me during my studies

ACKNOWLEDGEMENT

First and foremost, all praises be to Allah and to Him alone, thank Allah (Subhana Wataala) for endowing me with health, patience, and knowledge to complete this work. Words are insufficient to describe my gratefulness and appreciation to Him in the whole process of the preparation, compiling and writing of this thesis. I indebted to Allah for all the bounties. He bestowed on me to enable me to alhamdulillah successfully finish this study. Thank You Allah.

I would like to express my gratitude to my supervisor Asst.Prof. Nor Azwadi and co-supervisor Dr. Natrah Kamaruzaman for all their support, guidance and encouragement throughout this work. Without their fruitful discussions and comments through very regular research meetings, this work would not have been possible. They never forced me to follow their personal viewpoints but everything was opened for discussions.

I would like to thank the Ministry of Higher Education and Scientific Research, Iraq for providing doctoral scholarship for my study.

Finally, I would like to express my deepest gratitude to my father (May God have mercy on him), my mother, my wife, my brothers and sisters and all other relatives, for their emotional and moral support throughout my academic career and also for their love, patience, encouragement and prayers. Words fail to express my gratitude.

ABSTRACT

In recent years, the use of passive techniques to enhance heat transfer in microchannel heat sink (MCHS) has received increasing attention due to escalating demand for improved thermal management in modern electronic designs. However, most studies concentrated on the use of one type of passive techniques that focuses only on one aspect of its performance which is either to acquire high rate of heat transfer with higher pressure drop, or gain low pressure drop at low rate of heat transfer. For further enhancement of hydrothermal performance in MCHS, this research combined two techniques to exploit features of high heat transfer in lower pressure drop. Three new configurations developed were numerically investigated, and experimentally validated. To assess the effects of various geometrical parameters, an optimization technique was used to calculate the most efficient geometry of the proposed designs. The first configuration is a combination between wavy channel and secondary channels (WMSC) etched on the channels walls. The attributes of this configuration are manifested in enhancing the flow mixing within main channels by Dean vortices and among adjacent channels through secondary channels. The results showed that the new design of WMSC has enhanced the overall thermal performance by 140% as compared with the straight MCHS. The second configuration is a combination between a sinusoidal grooves and rectangular ribs installed in the central portion of the channel (MC-SCRR). The flow area enlargement provided by the cavities has significantly reduced the pressure drop caused by the ribs. Besides, this configuration contributes to increase the heat transfer by inducing flow jet impingement and vortices as well as increasing the contact surface area. This design has achieved an enhancement of 85% more than the straight MCHS. The final configuration uses a combination of secondary oblique channels in alternating direction and rectangular ribs (MC-SOCRR). The new design has exploited a larger flow area which is provided by the secondary channels to reduce pressure drop caused by ribs, and increased the flow mixing between the main channels. These features have contributed to enhance the performance of MC-SOCRR by 98% more than the straight MCHS.

ABSTRAK

Dalam tahun-tahun kebelakangan ini, penggunaan teknik pasif untuk meningkatkan pemindahan haba dalam saluran mikro penadah haba (MCHS) telah mendapat perhatian yang tinggi disebabkan oleh peningkatan permintaan untuk penambahbaikan pengurusan haba dalam reka bentuk elektronik moden. Walau bagaimanapun, kebanyakan kajian tertumpu kepada penggunaan satu jenis teknik pasif yang hanya memfokuskan kepada satu aspek prestasi yang sama ada untuk memperoleh kadar pemindahan haba yang tinggi dengan penurunan tekanan yang lebih tinggi atau untuk mendapatkan penurunan tekanan rendah pada kadar pemindahan haba yang rendah. Untuk mempertingkatkan lagi prestasi hidroterma dalam MCHS, kajian ini menggabungkan dua teknik untuk mengeksploitasi ciri-ciri pemindahan haba yang tinggi dalam penurunan tekanan yang lebih rendah. Tiga reka bentuk baru yang dibangunkan dikaji secara numerik dan disahkan secara eksperimen. Untuk menilai kesan pelbagai parameter geometri, teknik pengoptimuman telah digunakan untuk pengiraan geometri yang paling berkesan terhadap reka bentuk yang dicadangkan. Reka bentuk pertama adalah gabungan antara saluran beralun dan saluran sekunder (WMSC) terukir pada dinding saluran. Atribut reka bentuk ini ditunjukkan dalam meningkatkan aliran pencampuran dalam saluran utama oleh vorteks utama dan di antara saluran bersebelahan melalui saluran sekunder. Dapatan menunjukkan bahawa reka bentuk WMSC yang baharu telah meningkatkan prestasi haba keseluruhan sehingga 140% berbanding dengan MCHS lurus. Reka bentuk kedua adalah gabungan antara alur sinusoidal dan tulang rusuk segi empat tepat yang dipasang di bahagian tengah saluran (MC-SCRR). Pembesaran kawasan aliran yang disediakan oleh rongga telah mengurangkan penurunan tekanan yang disebabkan oleh tulang rusuk. Di samping itu, reka bentuk ini menyumbang dalam peningkatan pemindahan haba dengan mendorong pelepasan aliran jet dan vorteks di samping meningkatkan kawasan permukaan sentuhan. Reka bentuk ini telah mencapai peningkatan 85% lebih daripada MCHS lurus. Reka bentuk akhir menggunakan gabungan antara saluran serong sekunder dalam arah bergantian dan rusuk segi empat tepat (MC-SOCRR). Reka bentuk baru telah mengeksploitasi kawasan aliran yang lebih besar yang disediakan oleh saluran sekunder untuk mengurangkan penurunan tekanan yang disebabkan oleh tulang rusuk, dan meningkatkan aliran pencampuran antara saluran utama. Ciri-ciri ini telah menyumbang kepada peningkatan prestasi MC-SOCRR sebanyak 98% lebih daripada MCHS lurus.

TABLE OF CONTENT

CHAPTER	TITLE	PAGE
	DECLARATION	ii
	DEDICATION	iii
	ACKNOWLEDGEMENT	iv
	ABSTRACT	v
	ABSTRAK	v
	TABLE OF CONTENT	vii
	LIST OF TABLES	xiii
	LIST OF FIGURES	xv
	LIST OF ABBREVIATIONS	xxviii
	LIST OF SYMBOLS	xxxii
	LIST OF APPENDICES	xxxiii
1	INTRODUCTION	1
	1.1 Background of study	1
	1.2 Overview of heat transfer augmentation techniques	5
	1.2.1 Active method	6
	1.2.2 Passive method	6
	1.3 Heat transfer augmentation techniques in microchannel	6
	1.4 Problem statement	8

1.5	Objectives of the work	10
1.6	Scope	11
1.7	Chapter summery	12
2	LITERATURE REVIEW	13
2.1	Introduction	13
2.2	Corrugated channel	14
2.2.1	Dean vortices	14
2.2.2	Chaotic advection	17
2.3	Corrugated microchannel heat sink	19
2.3.1	Wavy microchannel heat sink	20
2.3.2	Zigzag microchannel heat sink	27
2.4	Flow disruption	31
2.4.1	Cavities in microchannel heat sink	33
2.4.2	Ribs in microchannel heat sink	39
2.4.3	Effect of ribs and grooves	41
2.4.4	Offset strip fins	48
2.5	Interrupted-wall channel	50
2.6	Research gaps	67
2.7	Chapter summary	67
3	RESEARCH METHODOLOGY	70
3.1	General overview	70
3.2	Wavy microchannel with oblique secondary channel in alternating orientation (WMSC)	73
3.2.1	Mathematical modeling of WMSC	73
3.2.2	Assumptions	76
3.2.3	Boundary conditions	76
3.2.4	Grid independence	78

3.3	Microchannel heat sink with sinusoidal cavities and rectangular ribs (MC-SCRR).	79
3.3.1	Mathematical modeling of microchannel heat sink	79
3.3.2	Boundary conditions	82
3.3.3	Grid independency	83
3.4	Microchannel heat sink with secondary oblique channels in alternating direction and rectangular ribs (MC-SOCRR)	85
3.4.1	Mathematical modeling of microchannel heat sink	85
3.4.2	Boundary condition	89
3.4.3	Grid independency	89
3.5	Governing equations	91
3.6	Solution algorithm	92
3.7	Data reduction	93
3.8	Experimental study	94
3.8.1	Test rig	94
3.8.2	Experimental procedures	99
3.8.3	The calibration of measuring instruments	100
3.8.4	Data reduction	103
4	RESULT AND DISCUSSION	110
4.1	Introduction	110
4.2	Wavy microchannel with oblique secondary channel in alternating orientation (WMSC).	111
4.2.1	The characteristic design of wavy microchannel with oblique secondary channel in alternating orientation (WMSC).	111
4.2.1.1	Velocity distribution	111
4.2.1.2	Dean vortices	119
4.2.1.3	Chaotic advection	121

4.2.1.4	Temperature distribution	122
4.2.1.1	Characteristics of pressure distribution	128
4.2.1.2	Performance analysis	131
4.2.2	The effect of geometrical parameters of wavy microchannel with secondary channel WMSC on hydrothermal performance	135
4.2.2.1	The effect of relative amplitude	135
4.2.2.2	The effect of relative secondary channel width	140
4.2.3	Experimental results	145
4.2.3.1	Uncertainty analysis of experimental results	145
4.2.3.2	Nusselt number	146
4.2.3.3	Average wall temperature	147
4.2.3.4	Pressure drop	149
4.3	Microchannel heat sink with sinusoidal cavities and rectangular ribs MC-SCRR.	150
4.3.1	Validation of rectangular microchannel (MC-RC) based on the conventional predictions.	150
4.3.2	Fluid flow and heat transfer characteristics in microchannel with sinusoidal cavities and rectangular ribs MC-SCRR.	153
4.3.2.1	Characteristics of velocity distribution	153
4.3.2.2	Characteristics of pressure distribution	156
4.3.2.3	Characteristics of temperature distribution	157
4.3.2.4	Performance analysis	159
4.3.3	The effect of geometrical parameters of rib and cavity on hydrothermal performance.	163

4.3.3.1	The effect of relative amplitude:	164
4.3.3.2	The effect of relative rib width	167
4.3.3.3	The effect of relative rib length	171
4.4	Microchannel heat sink with secondary oblique channels in alternating direction and rectangular ribs (MC-SOCRR)	175
4.4.1	Validation of rectangular microchannel (MC-RC) based on the conventional predictions.	175
4.4.2	Fluid flow and heat transfer characteristics of microchannel with secondary channels and rectangular ribs MC-SCRR.	178
4.4.2.1	Characteristics of velocity distribution	178
4.4.2.2	Characteristics of pressure distribution	180
4.4.2.3	Characteristics of temperature distribution	182
4.4.2.4	Performance analysis.	185
4.4.3	The effect of geometrical parameters of ribs and secondary channels on hydrothermal performance.	188
4.4.3.1	The effect of relative secondary channel width (λ).	188
4.4.3.2	The effect of relative rib width (β)	192
4.4.3.3	The effect of angle (θ)	195
4.5	The mechanism of reducing pressure drop in cavities and secondary channels.	198
4.6	The performance evaluation of new configurations in turbulent flow regime.	201
4.7	Comparison with related literature findings	205

4.8	Performance evaluation of the proposed designs.	208
5	CONCLUSION	209
5.1	Contributions	212
5.2	Suggestions for future work	213
	REFERENCES	214
	Appendices A-C	227-244

LIST OF TABLES

TABLE NO.	TITLE	PAGE
2.1	A summary of relevant literature on the effect of wavy MCHS on the heat transfer and pressure drop	31
2.2	A summary of relevant literature on the effect of corrugated channel parameters on the hydrothermal performance of MCHS	57
2.3	A summary of relevant literature on the effect of cavities on the hydrothermal performance of MCHS	60
2.4	A summary of relevant literature on the effect of ribs and cavities on the hydrothermal performance of MCHS	62
2.5	A summary of relevant literature on the effect of offset strip fins on the hydrothermal performance of MCHS	64
2.6	A summary of relevant literature on the effect of interrupted wall channel on the hydrothermal performance of MCHS	65
3.1	The dimensions of geometrical parameters of WMSC	75
3.2	Grid independency test	79
3.3	Geometrical parameters of SC-RR MCHS.	82
3.4	Grid independency test	84
3.5	Geometrical parameters of MC-SOCRR	88
3.6	Grid independency test.	91
4.1	Geometrical parameters of WMSC	135

4.2	Geometrical parameters of WMSC	141
4.3	Uncertainties of measured variables in experiments	146
4.4	The values of relative amplitude, relative rib width and relative rib length	164
4.5	Values of relative amplitude, relative rib width and relative rib length	168
4.6	Values of relative amplitude, relative rib width and relative rib length	172
4.7	The values of the relative secondary channel width (α), the relative rib width (β) and angle θ	188
4.8	The values of the relative secondary channel width (α), the relative rib width (β) and angle θ	192
4.9	Values of the relative secondary channel width (α), the relative rib width (β) and angle θ .	196
A.1	Thermocouple readings	229
A.2	Flow meter calibration data according to the manufacturer	231
A.3	Pressure transducer calibration data according to the manufacturer	232
B.1	Sample of data	236

LIST OF FIGURES

FIGURE NO.	TITLE	PAGE
1.1	The chronology of growth for three essential features in CPU design; transistor number per chip, clock speed and thermal design power. [3]	2
1.2	Recent applicati ^o n of microchannel heat sink in cooling of CPU (a) microchannel heat sink (b) installation of microchannel heat sink over CPU (c) tubes connection for water circulation.	3
1.3	Heat transfer augmentation method according to Steinke and Kandlikar [20].	8
2.1	(a) Schematic diagram of curved rectangular channel describing the effect of centrifugal force for the formation of Dean roll-cells, and (b) velocity streamlines of Dean roll-cells [28].	15
2.2	Schematic diagram describing the formation of Dean vortices in circular cross-section (a) when Dean number < critical Dean number, forming of pair of counter-rotating roll cells known as Dean roll-cells (b) when Dean number > critical Dean number, another pair of counter-rotating vortices called Dean vortices [31].	15
2.3	Flow visualization of curved rectangular channel with different aspect ratio describing the Dean roll-cells and DVs for: (a) AR = 0.5 and DN = 203 (b) AR = 1 and DN = 183 (c) AR = 2.5 and DN = 174 [32]	16

2.4	(a) Helical heat exchanger (b) regular Dean Flow in cross-section of helical heat exchanger.[43]	18
2.5	(a) Chaotic heat exchanger (b) schematic of bend which is rotated by 90° with respect to the neighbouring [43]	18
2.6	Reynolds number dependent thermal performance factor for helical and chaotic configurations [43]	19
2.7	The waviness dependent variation of temperature distribution and local Nusselt number along the MC for: (a) Increased waviness along the flow direction (b) Locally increased waviness in the middle. [6]	21
2.8	(a) Poincare sections obtained from particle tracking, and (b) DVs at section 5L for wavy channel with $A = 259 \mu\text{m}$ at $\text{Re} = 600$ [48]	22
2.9	(a) Comparison of pressure drop versus thermal resistance for; two type of transverse MCHS (transverse wavy channel DN1, transverse wavychannel 2), two types of longitudinal MCHS(longitudinal wavy channel1, longitudinal wavy channel2) and straight rectangular MCHS, (b) Generic structure of transverse wavy channel (c) Generic structure of LWC [51]	24
2.10	Velocity vectors in: (a) serpentine wavy MCHS, (b) raccoon wavy MCHS[54]	25
2.11	(a) Geometrical parameters of CD-MCHS S(aspect-ratio), λ (waviness)and γ (expansion factor) (b) Wavelength dependent variation of Nusselt number for different aspect ratio (0.5-2) at Reynolds number of 600 (c) Wavelength dependent variation of performance factor for different aspect ratio (0.5-2) at Reynolds number of 600. [2]	26
2.12	Streamline plots at the upper furrow of the channel for: (a) sinusoidal CD-MCHS, and (b) constant curvature CD-	

	MCHS at different amplitude ratios (A/L) with $Re = 100$ [55].	27
2.13	Performance factor for sinusoidal and constant curvature CD-MCHS for different amplitude ratios with $Re = 50, 100, 150,$ and 200 [55]	28
2.14	Lz/d dependent variation of (a) heat transfer enhancement factor e_{Nu} and (b) pressure drop penalty factor e_f . [44].	29
2.15	Rc/d dependent variation of (a) heat transfer enhancement factor e_{Nu} and (b) pressure drop penalty factor e_f . [44].	29
2.16	Bend angle (θ) dependent variation of (a) heat transfer enhancement factor e_{Nu} and (b) pressure drop penalty factor e_f . [44]	30
2.17	(a) Interferogram of temperature distribution in plate heat exchanger channel with hemi-cylindrical ribs for different Reynolds number (500, 1500, 2500, and 5000) and (b) Channel length dependent variation of local Nusselt number [71]	32
2.18	(a) Holographic image of temperature distribution in grooved channel with profiled surface for various Reynolds number (462, 925, and 1619) and (b) Local Nusselt number as a function of channel length [72]	33
2.19	(a) Streamlines along the mid-plane of the working fluid height and (b) Flow velocity along the middle of the working fluid height [73].	34
2.20	Geometrical parameters of fan-shaped reentrant cavities [73]	34
2.21	The schematic of three configurations of the MCs. [76]	35
2.22	Comparison of the numerical predictions and experimental data in conventional rectangular MCHS(R), MCHS with triangular reentrant cavities (T) and MCHS with fan shape	

	reentrant cavities (F) for (a) Average Nusselt number as a function of Reynolds Nu and (c) $f_{app}Re$ [76].	36
2.23	Geometrical parameters of the trapezoidal GMCHS. [83]	39
2.24	(a) Magnitude of flow velocity and (b) Streamlines distribution along the central plain ($z = 0.25$ mm) between fan-shaped reentrant cavities MCHS ($e/Dh = 0.1553$) and rectangular MCHS at $Re = 199.5$ [88].	43
2.25	(a) Variation of thermal enhancement factor with Reynolds number and (b) Geometrical parameters of fan-shaped reentrant cavities MCHS [88]	43
2.26	Reynolds number dependent variation of (a) thermal efficiency η , (b) Entropy generation number Ns , (c) Synergy number Fc for four types of MCHS ; fan-shaped reentrant cavities with circular ribs(F-C), fan-shaped reentrant cavities with trapezoidal ribs(F-Trp), fan-shaped reentrant cavities with rectangular ribs(F-R) and fan-shaped reentrant cavities with triangular ribs(F-Tri) [89].	44
2.27	Schematic diagram of cavities and ribs arrangement (a) Tri.C-C.R, (b) Tri.C-Tri.R, (c) Tri.C-Tra.R, (d) Tra.C-C.R, (e) Tra.C- Tri.R and (f) Tra.C-Tra.R. [90].	45
2.28	Reynolds number dependent variation of overall performance for cavity-rib arrangement MCHS [90].	46
2.29	Streamlines and temperature contour at $Re = 500$ (a) Groove on one surface, (b) Obstacle on one surface and groove on opposite surface, (c) Obstacle on one surface, (d) Obstacles are arranged at opposite surface, (e) Grooves and obstacles are staggered on both surfaces, and (f) Grooves and obstacles are aligned on both surfaces. [91].	47
2.30	The functionality of offset-fin strips which work to split the flow and deviate its direction to spread over the entire region [94].	49

2.31	The distribution of (a) velocity, (b) vorticity and (c) temperature at the midplain in MCHS with offset strip fins [98]	50
2.32	(a) The geometry of interrupted MCHS (b) Local Nusselt number versus non-dimensional flow length for rectangular MCHS and interrupted MCHS (c) Pressure distribution along flow direction for rectangular MCHS and interrupted MCHS. Ref. [101].	52
2.33	Streamlines and velocity distributon for (a)interrupted microchannel with rib (b) interrupted microchannel without rib (c) stright channel [102]	53
2.34	Schematic of a louvered-fin array [105]	54
2.35	MCHS with obique fins [103]	54
2.36	Comparison of pressure drop in MCHS having oblique fin with conventional MC [103]	55
3.1	Framework of current study	72
3.2	Geometrical parameters of one WMSC (a) basic parameters, (b) total length (Lt), channel height (Hc) and substrate thickness (t).	74
3.3	(a) Top view of WMSC, (b) Top view of computational domain of WMSC used in current study.	75
3.4	The boundary conditions which applied on WMSC.	76
3.5	3-D mesh structure the WMSC.	78
3.6	(a) Schematic diagrams of MC-SCRR (b) geometric parameters of MC-SCRR.	80
3.7	(a) Schematic diagrams of MC-RC. (b) geometric parameters of MC-RC.	81
3.8	(a) Three dimensional geometry of MC-SCRR with mesh (b) Computational grid in the x-z plane of MC-SCRR with $\beta=0.333$, $\lambda=0.15$ and $\Gamma=0.4$.	84

3.9	(a) Schematic diagrams of MC-SOCRR (b) geometric parameters of MC-SOCRR.	86
3.10	(a) Schematic diagrams of MC-RC (b) geometric parameters of MC-RC.	87
3.11	Variation of secondary channel orientation with angle θ	87
3.12	Three dimensional mesh structure of microchannel heat sink with ribs and secondary channels	90
3.13	Main parts of the test section.	95
3.14	Top view of real test rig geometry	95
3.15	Front view of real test rig geometry	96
3.16	Manifold geometry (a) Top view (b) T-T cross-section.	96
3.17	The photo of real geometry of WMSC (a) Top surface shows the microchannels arrangement (b) The upper part of copper block.	97
3.18	(a) Geometry of copper block (b) Transparent geometry of copper block to show all holes	98
3.19	Schematic diagram of flow loop	99
3.20	Experimental system and instruments used in testing	100
3.21	Starting of heating WMSC	101
3.22	Transient temperature readings	101
3.23	Steady state temperature readings	102
3.24	Pressure transducer reading	102
3.25	The positions of thermocouples in copper block.	105
3.26	Section view of manifold and MCHS shows the flow trajectory through different regions.	108
4.1	Velocity vector distribution in various cross-sections along (a) RMCHS,(b) WMCHS and (c) WMSC, on x-z plane at $y=0.3\text{mm}$ and $Re=200$.	112

4.2	Velocity streamlines along (a) RMCHS, (b) WMCHS and (c) WMSC, on x-z plane at $y=0.3\text{mm}$ and $Re=200$.	113
4.3	Velocity contours along (a) RMCHS, (b) WMCHS and (c) WMSC, on x-z plane at $y=0.3\text{mm}$ and $Re=200$. All velocities units in m/sec	115
4.4	Velocity vector distribution in various cross-sections along (a) RMCHS,(b) WMCHS and (c) WMSC, on x-z plane at $y=0.3\text{mm}$ and $Re=600$	116
4.5	Velocity streamlines along (a) RMCHS, (b) WMCHS and (c) WMSC, on x-z plane at $y=0.3\text{mm}$ and $Re=600$.	117
4.6	Velocity contours along (a) RMCHS, (b) WMCHS and (c) WMSC, on x-z plane at $y=0.3\text{mm}$ and $Re=600$. All velocities units in m/s	118
4.7	Dean vortices in WMCHS	119
4.8	The development of Dean vortices with Reynolds number (200-800).	120
4.9	The interaction of secondary flow with Dean vortices in WMSC	121
4.10	The temperature distribution contours for the (a) RMCHS,(b) WMCHS and (c) WMSC on x-z plane at $y=0.25\text{mm}$ with $Re=200$.	123
4.11	The temperature distribution contours for the (a) RMCHS,(b) WMCHS and (c) WMSC on x-z plane at $y=0.25\text{mm}$ with $Re=600$.	124
4.12	Temperature contours describing the thermal boundary layer in vertical section of WMCHS at ($x=0.01\text{m}$) for (a) $Re=200$, (b) $Re=600$.	126
4.13	Temperature contours describing the thermal boundary layer in vertical section of WMSC at ($x=0.01\text{m}$) for (a) $Re=200$, (b) $Re=600$.	127

4.14	Average base temperature versus Reynolds number for RMCHS, WMCHS, and WMSC.	128
4.15	The pressure distribution contours for the (a) RMCHS,(b) WMCHS and (c) WMSC on x-z plane at $y=0.25\text{mm}$ with $Re=200$.	129
4.16	The pressure distribution contours for the (a) RMCHS,(b) WMCHS and (c) WMSC on x-z plane at $y=0.25\text{mm}$ with $Re=600$.	130
4.17	Pressure drop along channel length for WMCHS and WMSC	131
4.18	Friction factor ratio versus Reynolds number for WMSC and WMCHS.	132
4.19	Nusselt number ratio versus Reynolds number for WMSC and WMCHS.	133
4.20	Variation of performance factor Pf with Reynolds number for WMSC and WMCHS.	134
4.21	Variation of average friction factor f_{ave} with relative amplitude λ for WMSC at relative width $\alpha = 0.5$.	137
4.22	Variation of average Nusselt number Nu_{ave} with relative amplitude λ for WMSC at relative width $\alpha = 0.5$.	137
4.23	The pressure distribution contours for the WMSC for relative amplitudes ranged from 0.025-0.1 on x-z plane at $y=0.25\text{mm}$ with $Re=600$.	138
4.24	The temperature distribution contours for the WMSC for relative amplitudes ranged from 0.025-0.1 on x-z plane at $y=0.25\text{mm}$ with $Re=600$.	139
4.25	Variation of performance factor Pf with relative amplitude λ for WMSC at relative width $\alpha=0.5$.	140
4.26	Variation of flow rate percentage through secondary channels versus α .	141

4.27	Variation of average friction factor f_{ave} with relative width α for WMSC at relative amplitude $\lambda=0.05$.	142
4.28	Flow streamlines in WMSC with various relative width describe the flow recirculation in secondary channels.	143
4.29	Variation of average Nusselt number Nu_{ave} with relative width α for WMSC at relative amplitude $\lambda=0.05$.	144
4.30	Variation of performance factor Pf with relative width α for WMSC at relative amplitude $\lambda=0.05$.	144
4.31	Experimental results of Nusselt number for WMSC versus Reynolds number ranged $200 < Re < 620$.	147
4.32	Comparisons between numerical and experimental results of Nusselt number for WMSC	148
4.33	Comparisons between numerical and experimental results of average wall temperature for WMSC.	148
4.34	Experimental results of pressure drop for WMSC versus Reynolds number ranged $200 < Re < 620$.	149
4.35	Comparisons between numerical and experimental results of pressure drop for WMSC versus Reynolds number ranged $200 < Re < 620$.	150
4.36	Numerical validation (a) local Nusselt number according to Philips [119] (b) Poiseuille number, and (c) Pressure drop according to Steinke & Kandlikar[4].	152
4.37	Streamline and velocity distribution for various structures on x-z plane ($y=0.25\text{mm}$) at $Re=200$.	154
4.38	Streamline and velocity distribution for various structures on x-z plane ($y=0.25\text{mm}$) at $Re=500$.	155
4.39	Streamlines and velocity distribution in z-y plane at $x=5\text{mm}$ describes the transverse flow motion towards cavity depth.	156
4.40	Pressure distribution contours for the four types of MC's on x-z plane at $y=0.25\text{mm}$ with $Re=500$	157

4.41	Temperature distribution contours for the four types of MC's on x-z plane at $y=0.25\text{mm}$ with $Re=500$	159
4.42	Average temperature of the bottom surface of MC-RC, MC-SC, MC-RR and MC-SCRR.	160
4.43	The surface area of the four types of MC's	160
4.44	Variation of friction factor ratio with Reynolds number for MC-SCRR, MC-RR and MC-SC.	161
4.45	Variation of Nusselt number ratio with Reynolds number for MC-SCRR, MC-RR and MC-SC.	161
4.46	Variation of performance factor Pf with Reynolds number for MC-SCRR, MC-RR and MC-SC.	163
4.47	Variation of average friction factor f_{ave} with relative amplitude λ for MC-SCRR at relative rib width $\beta=0.333$ and relative rib length $\Gamma=0.4$.	165
4.48	Variation of average Nusselt number Nu_{ave} with relative amplitude λ for MC-SCRR at relative rib width $\beta=0.333$ and relative rib length $\Gamma=0.4$.	166
4.49	Temperature distribution and streamlines in MC-SCRR at $Re=600$ of (a) $\lambda=0.05$ (b) $\lambda=0.15$.	166
4.50	Variation of performance factor Pf with relative amplitude λ for MC-SCRR at relative rib width $\beta=0.333$ and relative rib length $\Gamma=0.4$.	167
4.51	Variation of average friction factor f_{ave} with relative rib width β for MC-SCRR at relative cavity amplitude $\lambda=0.15$ and relative rib length $\Gamma=0.4$.	169
4.52	Pressure distribution and streamlines in MC-SCRR at $Re=600$ of (a) $\beta=0.3$ (b) $\beta=0.6$.	169
4.53	Variation of average Nusselt number Nu_{ave} with relative rib width β for MC-SCRR at relative cavity amplitude $\lambda=0.15$ and relative rib length $\Gamma=0.4$.	170

4.54	Variation of performance factor Pf with relative rib width β for MC-SCRR at relative cavity amplitude $\lambda=0.15$ and relative rib length $\Gamma=0.4$.	171
4.55	Pressure distribution and streamlines in MC-SCRR at Re=600 of (a) $\Gamma=0.5$ (b) $\Gamma=0.8$.	172
4.56	Variation of average friction factor f_{ave} with relative rib length Γ for MC-SCRR at $\lambda=0.15$ and $\beta=0.3$.	173
4.57	Variation of average Nusselt number Nu_{ave} with relative rib length Γ for MC-SCRR at $\lambda=0.15$ and $\beta=0.3$.	174
4.58	Variation of performance factor Pf with relative rib length Γ for MC-SCRR at relative cavity amplitude $\lambda=0.15$ and relative rib width $\beta=0.3$	175
4.59	Numerical validation (a) local Nusselt number according to Philips [119] (b) Poiseuille number, and (c) Pressure drop according to Steinke & Kandlikar[4].	177
4.60	Streamline and velocity distribution for various structures on x-z plane ($y=0.25\text{mm}$) at Re=300.	179
4.61	Flow streamlines distribution in three-dimensional of MC-SOCRR with the second half mirrored at symmetrical line	180
4.62	The pressure distribution contours for the four types of MC's on x-z plane at $y=0.25\text{mm}$ with Re=300.	181
4.63	Temperature distribution contours for the four types of MC's on x-z plane at $y=0.25\text{mm}$ with Re=300.	183
4.64	Variation of average temperature of the bottom surface of MC-RC, MC-SC, MC-RR and MC-SCRR.	184
4.65	Variation of temperature difference between channel walls and water for all types of MCHS.	184
4.66	Variation of Nu/Nu_0 versus Reynolds number for MC-SOCRR, MC-RR and MC-SOC.	185

4.67	Variation of f/f_0 versus Reynolds number for MC-SOCRR, MC-RR and MC-SOC.	186
4.68	Variation of performance factor Pf with Reynolds number for MC-SOCRR, MC-RR and MC-SOC.	187
4.69	Variation of average friction factor f_{ave} with relative secondary channel width α for MC-SOCRR at $\beta=0.5$, and $\theta = 45^\circ$.	189
4.70	Variation of average Nusselt number Nu_{ave} with relative secondary channel width α for MC-SOCRR at $\beta=0.5$ and $\theta =45^\circ$.	190
4.71	Temperature distribution contours for different value of α on x-z plane at $y=0.25\text{mm}$ with $Re=300$.	191
4.72	Variation of performance factor with relative secondary channel width α for MC-SOCRR at $\beta=0.5$ and $\theta =45^\circ$.	191
4.73	Variation of average Nusselt number Nu_{ave} with relative rib width β for MC-SOCRR at $\alpha=0.666$ and $\theta =45^\circ$.	193
4.74	The effect of rib width on temperature distribution in MC-SOCRR of (a) $\beta=0.3$ (b) $\beta=0.6$	194
4.75	Variation of average friction factor f_{ave} with relative rib width β for MC-SOCRR at $\alpha=0.666$ and $\theta =45^\circ$.	194
4.76	Variation of performance factor Pf with relative rib width β for MC-SOCRR at $\alpha=0.666$ and $\theta =45^\circ$.	195
4.77	Variation of average Nusselt number Nu_{ave} with angle θ for MC-SOCRR at $\alpha=0.666$ and $\beta = 0.5$.	196
4.78	Flow streamlines in MC-SOCRR with angle of ($\theta=75$)	197
4.79	Variation of average friction factor f_{ave} with angle θ for MC-SOCRR at $\alpha=0.666$ and $\beta = 0.5$.	197
4.80	Variation of Performance factor Pf with relative angle θ for MC-SOCRR at $\alpha=0.666$ and $\beta = 0.5$.	198

4.81	Pressure drop along MC-SCRR	199
4.82	Pressure drop along MC-SOCRR	200
4.83	Pressure drop along MC-SCRR	200
4.84	(a) Friction factor ratio, (b) Nusselt number ratio and (c) performance factor for WMSC in laminar and turbulent regions	202
4.85	(a) Friction factor ratio, (b) Nusselt number ratio and (c) performance factor for MC-SCRR in laminar and turbulent regions	203
4.86	(a) Friction factor ratio, (b) Nusselt number ratio and (c) Performance factor for MC-SOCRR in laminar and turbulent regions	204
4.87	Comparison between new design of WMSC and the literature findings that use single passive technique.	206
4.88	Comparison between new designs of MC-SCRR and MC-SOCRR with the literature findings that use single passive technique.	207
A.1	Thermocouple calibration process	228
A.2	Calibration curves of (a) thermocouple probe no.1, (b) thermocouple probe no.2, (c) thermocouple probe no.3, (d) thermocouple probe no.4 and (e) thermocouple probe no.5	230
A.3	Calibration curves of flow-meter	232
A.4	Calibration curves of pressure transducer	233
A.5	Schematic diagram for the system which used in verification of pressure transducer calibrations	234
C.1	Cover dimensions	240
C.2	(a),(b)and (c) manifold dimensions	242
C.3	(a)&(b) Copper block dimensions	243
C.4	Base dimensions	244

LIST OF ABBREVIATIONS

Abbreviations

A	-	Amplitude
A_B	-	Base area
A_{bot}	-	Un-finned surface area
A_c	-	Fin cross sectional area
$A_{conv.}$	-	Convection heat transfer area
A_{film}	-	Film area
A_{fin}	-	Fin area
AR	-	Aspect Ratio (width/height)
CA	-	Chaotic advection
CC	-	Corrugated channel
CD-MCHS	-	Convergent-divergent microchannel heat sink
C_{pf}	-	Fluid specific heat
D_h	-	Hydraulic diameter
DN	-	Dean number
DN_C	-	Critical Dean Number
DVs	-	Dean vortices
f_{app}	-	Apparent friction factor
FD	-	flow disruption
FF	-	Friction factor

GMCHS	-	Grooved microchannel heat sink
h_{ave}	-	Average heat transfer coefficient
H_c	-	Channel height
k_{cu}	-	<i>Thermal conductivity of copper</i>
k_f	-	Thermal conductivity of the fluid
Kn	-	Knudsen number
k_s	-	Thermal conductivity of solid
L	-	Wave length
L_C	-	Cavity length
L_r	-	Rib length
L_t	-	Total length
MC	-	Microchannel
MCHS	-	Microchannel Heat Sink
MC-RC	-	Straight rectangular microchannel
MC-RR	-	Microchannel heat sink with rectangular ribs
MC-SCRR	-	Microchannel heat sink with sinusoidal cavities and rectangular ribs
MC-SOC	-	Microchannel heat sink with oblique channels in alternating direction
MC-SOCRR	-	Microchannel heat sink with secondary oblique channels in alternating direction and rectangular ribs.
Nu	-	Nusselt number
P	-	Perimeter
p	-	pressure
PD	-	Pressure drop
P_{in}	-	inlet pressure
P_{out}	-	Outlet pressure
Q	-	Volume flow rate

q	-	Heat flux
q''	-	Heat flux per unit area
Re	-	Reynolds number
RMCHS	-	Rectangular microchannel heat sink
t		Base thickness
T_f	-	Fluid temperature
T_{fave}	-	Average fluid temperature
T_{HS}	-	Heat sink temperature
T_{in}	-	Inlet temperature
T_{out}	-	Outlet temperature
Tra.C- Tri.R	-	Trapezoidal-cavities with triangular-rib
Tra.C-C.R	-	Trapezoidal-cavities with circular-rib
Tra.C-Tra.R	-	Trapezoidal-cavities with trapezoid-rib
Tri.C-C.R	-	Triangular-cavities with circular-rib
Tri.C–Tra.R	-	Triangular-cavities with trapezoidal-ribs
Tri.C-Tri.R	-	Triangular-cavities with triangular-rib
T_s	-	Solid temperature
T_w	-	Wall temperature
T_{wave}	-	Average wall temperature
T_{wi}	-	Inlet water temperature
T_{wo}	-	Outlet water temperature
u	-	Velocity component in x-direction
u_m	-	Mean velocity
v	-	Velocity component in y-direction
w	-	Velocity component in z-direction
W_c	-	Channel width

WMHS	-	Wavy microchannel heat sink
WMSC	-	Wavy microchannel with oblique secondary channel in alternating orientation
W_r	-	Rib width
W_s	-	Secondary channel width
W_t	-	Total width
W_w	-	Channel wall width
ZMCHS	-	Zigzag microchannel heat sink
TWC	-	Transverse wavy channel
LWC	-	Longitudinal wavy channel

LIST OF SYMBOLS**Symbols**

μ_f	-	Fluid viscosity
α	-	Relative secondary channel width
β	-	Relative rib width
Γ	-	Relative rib length
Δp	-	Pressure drop deference
η	-	Fin efficiency
θ	-	Angle of inclination
λ	-	Relative amplitude
ρ_f	-	Fluid density

LIST OF APPENDICES

APPENDIX	TITLE	PAGE
A	Calibration	227
B	Uncertainty	235
C	Drawings of apparatus parts	240

CHAPTER 1

INTRODUCTION

1.1 Background of study

Lately, rapid growth in the electronic industry has witnessed ultra-large-scale-integrated-circuit (ULSIC) as new generation high performing dense chip packages. However, such miniaturization causes the production of highly concentrated heat flux. This heat flux that raises the substrate temperature and creates hot spots is detrimental for the devices unless overcome. Any failure of removing such a high heat flux accelerates the meantime to failure (MTTF) and shorten the lifespan of electronic devices or even permanent damage [1]. Thus, appropriate thermal management of microelectronics is prerequisite to surmount the heat flux related damages. This considered to be the major obstacle towards further development of integrated electronic technologies. According to the international technology roadmap for semiconductors (ITRS), the peak power consumption of high- and low- performance integrated chips is expected to increase by 96% (147-288 W) and 95% (91-158 W) in 2016, respectively. The estimated amount of heat that need to be removed from the new 14 nm chip is higher than 100 W/cm^2 [2]. Figure 1.1 shows the chronology of growth for three essential features in CPU design; transistor number per chip, clock speed and thermal design power. It is clearly seen that the growth of thermal design power is closely related with increase of both clock speed and number of transistors per chip. This trend implies that any development in CPU design is associated with increase in the thermal fluxes at chip level.

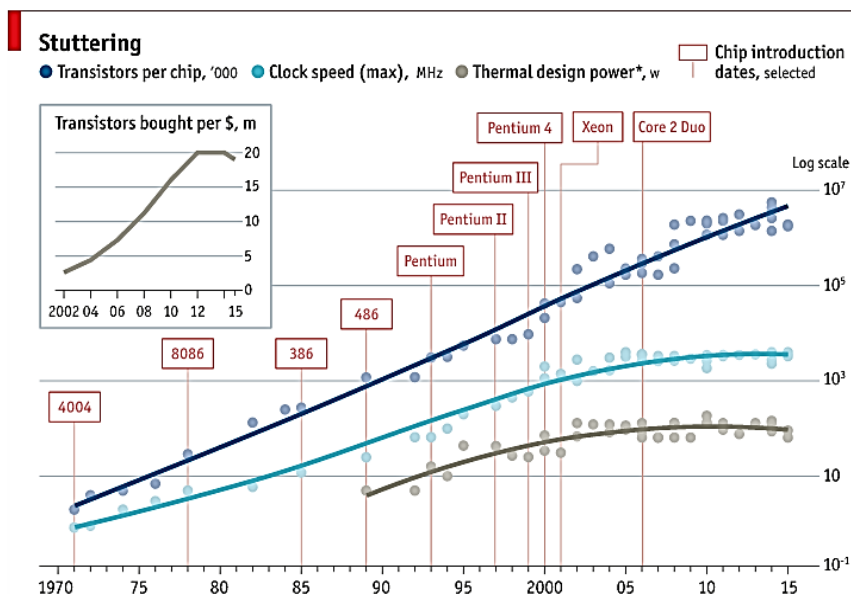


Figure 1.1: The chronology of growth for three essential features in CPU design; transistor number per chip, clock speed and thermal design power. [3]

Earlier, air-cooling method is extensively used for heat removal from integrated circuits due to its several attractive features such as low initial cost, high reliability, low operating maintenance cost, and high compatibility with micro-electronic environment [4]. However, with the rapid increase in power density and miniaturization of electronic packages this method became limited to satisfy the cooling demands. Use of various liquids as an alternative to air is proposed due to their high specific heat capacity and heat transfer coefficient. Several micro cooling methods are developed including micro-jet impingement, micro-heat pipe, micro-electro-hydrodynamic and microchannel heat sink MCHS. Among different micro-cooling methods the microchannel heat sink MCHS is appeared to be most prospective, which can remove heat at very high rate up to 790 W/cm^2 [5]. The central concept of microchannel (MC) is relying on its ability to provide the large heat transfer surface-to-volume ratio. MCs are used for two types of cooling such as single-phase and two-phase. Single-phase being easy for implementation is often used to remove intermediate heat fluxes. Figure 1.2 shows the recent application of MCHS in cooling of CPU. Although the two-phase can remove higher heat flux but it involves complex issues such as condensation, critical heat flux, saturation temperature, nucleation site activation etc. [6].

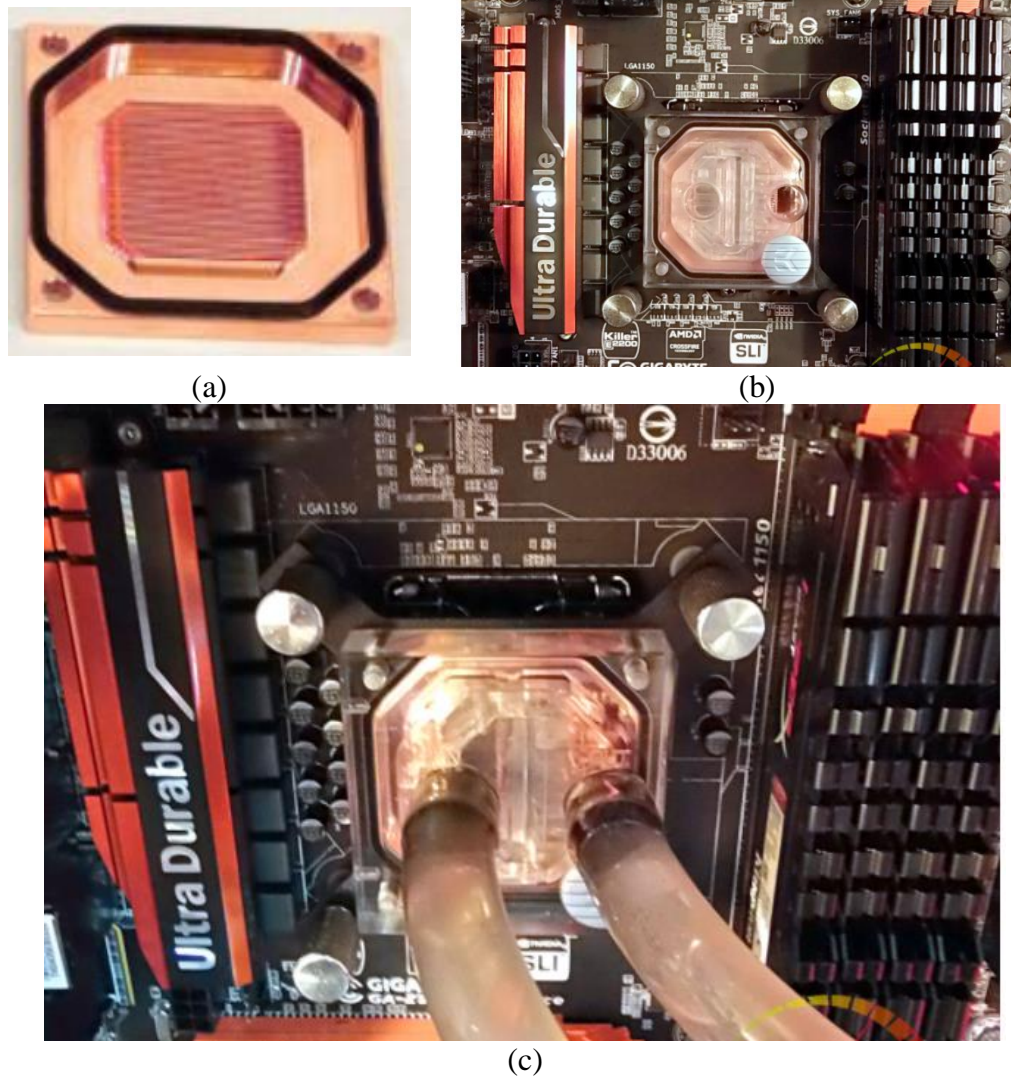


Figure 1.2: Recent application of microchannel heat sink in cooling of CPU (a) microchannel heat sink (b) installation of microchannel heat sink over CPU (c) tubes connection for water circulation.

The flow in conventional straight MCHS is predominantly within laminar flow regime because of the tiny size of the channels, which does not allow the flow to transit to the turbulent regime. Besides, in the conventional straight MCHS the accumulation of hotter fluid at the channel wall and cooler fluid along the channel core due to continuous growth of thermal boundary layer degrades the heat transfer in MCHS. Most of the early studies tried to improve the thermal performance of conventional straight rectangular MCHS by manipulating channel aspect ratio, channel length and wall thickness [7-10]. Some researchers manipulated the cross-section shape of

microchannel (e.g. circular, triangular, and trapezoidal) [11-16] for the performance enhancement. Alfaryjat et al. [17] studied numerically the influence of geometrical parameters on the thermal performance of microchannel, where three cross-section channel shapes including hexagonal, circular and rhombus are considered. Hexagonal cross-section revealed the highest pressure drop and heat transfer coefficient. Channel with rhombus cross-section exhibited highest value of friction factor and thermal resistance. Gunnasegaran et al. [18] examined the effect of varying cross-sectional shapes (rectangular, trapezoidal and triangle) on the hydrothermal performance of MCHS. Rectangular shape channel displayed maximum heat transfer augmentation followed by trapezoidal and triangular MCHS.

Despite the implementation of complex cross-sectional shapes, a precise geometry for disrupting the thermal boundary layer beyond the entrance region and subsequent achievement of enhanced hydrothermal performance is yet to be developed. An optimized strategy is needed to overcome the continuous heat generation due to excessive power consumption by high-performing integrated chips. Researchers took the advantages of heat transfer augmentation methods of conventional channels and applied them in MCHS. Tao et al. [19] suggested three strategies for the single-phase heat transfer enhancement such as reduction of the thermal boundary layer thickness, increase of both flow disruptions and velocity gradient near the heated surface. To promote heat transfer in MCHS, Steinke and Kandlikar [20] and Kandlikar and Grande [4] developed several techniques such as increase of surface area and heat transfer coefficient using interrupted and staggered strip-fin design, increase of local heat transfer coefficient by breaking boundary layer through periodic construction, incorporation of grooves and ridges, and incorporation of mixing features to improve the mixing flow.

1.2 Overview of heat transfer augmentation techniques

The study of heat transfer augmentation became the focus of attention since 1920 until the present time. In 1980, the advantages of this study began to emerge within the industrial applications [21]. Most of these researches included the conventional sizes of pipes and channels which used in heat exchangers and other thermal applications. Many researchers have presented reviews of the state of art. Bergles is one of these researchers who presented many reviews in this topic as in [21-23]. The author has classified the heat transfer augmentation methods into two kinds; passive and active. Tao et al.[19] suggested three strategies for the single-phase heat transfer enhancement. These strategies are; reducing the thermal boundary layer thickness, increasing flow disruptions and increasing velocity gradient near the heated surface. Dewan et al. [24] presented a review of passive heat augmentation techniques which used in conventional pipes and ducts. The review focused on two kinds of inserts which placed inside pipes and ducts; twisted tape and wire coil. They observed that twisted tape inserts perform better in a laminar flow than turbulent because these inserts increase the mixing of the bulk flow. On the other hand, they found that wire coil enhances heat transfer in both laminar and turbulent flow, but it performs better in turbulent flow. Leal et al [25] reviewed the main techniques for the enhancement of heat transfer for both single-phase and two-phase flow system. The commonly used passive techniques was reviewed briefly while active methods were reviewed in detail. The researchers focused on the techniques that use periodic deformation of channel wall over time which can be achieved by using of the piezoelectric materials. These techniques found to be more applicable for microchannel system. In single-phase system, imposing a distortion traveling wave to a microchannel wall leads to an enhancement in both heat transfer and fluid motion. While in two-phase, and because of boiling in narrow space, both boiling and cavitation phenomena are involved in nucleation process.

1.2.1 Active method

This method encompasses using some of external power input for the system to enhance heat transfer. The sophisticated design is the characteristic of this method due to the modifications required that accompanies the external power sources. The active method includes many techniques such as vibration, electrostatic field, magnetic field and flow pulsation.

1.2.2 Passive method

This method does not require any external power input. The additional power needed is extracted from the system itself through manipulation in the geometrical parameters which in most cases causes further pressure drop. The researchers have been striving for improve thermal performance and reduced pressure drop to promote the overall hydrothermal performance. A good microchannel heat sink design should have efficient thermal performance with minimum entropy generation. This can be achieved through performing an optimization process to the geometrical parameters. The passive method includes many techniques such as surface roughness, flow disruptions, channel curvature, re-entrant obstructions, secondary flow and fluid additives.

1.3 Heat transfer augmentation techniques in microchannel

Most researches that involving heat transfer enhancement techniques in MCHS tend to use passive techniques more than active techniques due to the simplicity in design. Besides, it does not require any external power which may involve using special geometrical configurations. Steinke and Kandlikar [20] presented a first review that includes a comprehensive description about the applicability of heat transfer

enhancement techniques for single-phase flows in microchannels and minichannels. They classified these techniques into two categories; active and passive. Each category includes various techniques as in Figure 1.3. Tullius et al. [26] reviewed different techniques used in efforts to modify MCHS in both single- and two-phase laminar flow. Some surface modifications discussed include adding micro-fins, adding grooves, increasing surface roughness, etc. They also focused on characteristics of using Carbon nanotubes (CNT) in the structure of MCHS to improve thermal performance due to the high thermal conductivity. Dewan et al. [27] Conducted a comprehensive review of flow disruption in microchannel. They demonstrated the recent researches of using flow disruption techniques in microchannel.

Most studies are striving to enhance overall performance in MCHS which involve achieving two simultaneous objectives; increasing heat transfer rate with lower pressure drop. These two objectives can be accomplished using suitable technique which associated with optimization analysis for the effective geometrical parameters. The attributes of enhancement techniques are manifested through manipulation and modification in microchannel geometry which aim to:

- 1- Increase of surface area and heat area coefficient using interrupted and staggered strip-fin design.
- 2- Increase of local heat transfer coefficient by breaking boundary layer through periodic construction, incorporation of grooves and ridges, and incorporation of mixing features to improve the mixing flow.
- 3- Increase of mixing flow through promoting the chaotic advection and Dean vortices by using channel wavy microchannel.
- 4- Increase of mixing flow between adjoining channels through incorporation periodic secondary channels.

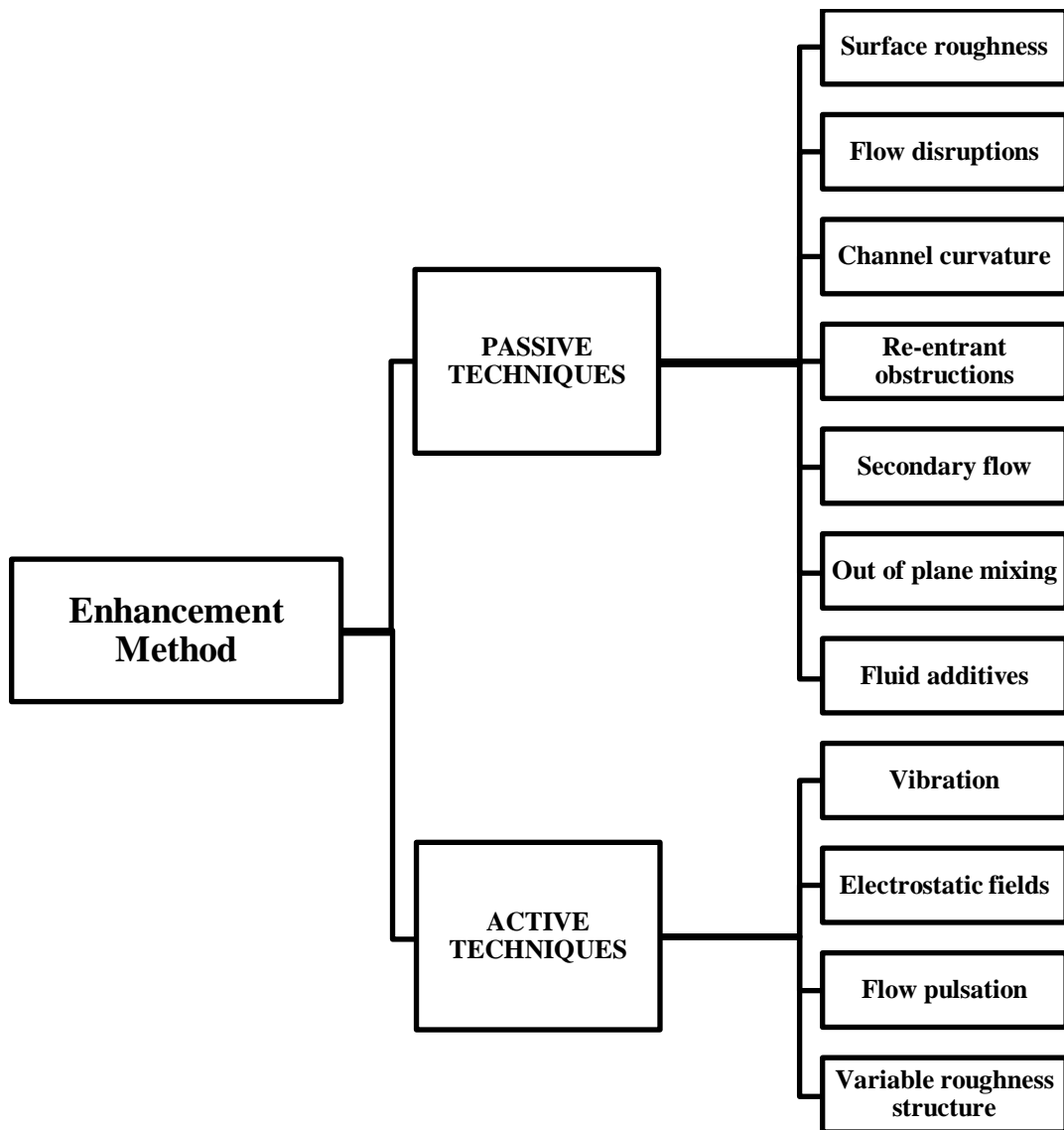


Figure 1.3: Heat transfer augmentation method according to Steinke and Kandlikar [20].

1.4 Problem statement

Since the invention of microchannel heat sink, a lot of numerical and experimental studies have been dedicated to investigating the characteristics of heat transfer and fluid flow in straight rectangular microchannel. There are many restrictions that hinder the improvement of thermal performance in straight simple

microchannel. The high pressure drop across the microchannel is one of the most significant limitations because it contributing in increasing pumping power consumption and leakage risk. Additionally, the micro size of the channels makes the flow invariably in laminar region, thus leads to low performance compared with turbulent flow. As consequences of the continuous increase in heat loaded and rigorous requirement of temperature determination for electronic elements, the straight simple channel is unable to satisfy these demands. So, a lot of studies have diverted the interest towards passive techniques which applied in conventional channels to be utilized in microchannel. Steinke and Kandlikar [20] proposed several techniques which are enforceable in microchannels to enhance heat transfer in microchannel such as incorporation of mixing features to improve the mixing flow , increase local heat transfer coefficient by breaking boundary layer, utilizing intermittent construction , incorporation of grooves , ribs and channel curvature .

Accordingly, many studies have adopted these strategies to improve the thermal performance of microchannel heat sink. Many investigations have been studied the single effect of different shapes, sizes or orientations of the groove, cavity, fins and ribs periodically attached to the side wall. The literature review is also showed that the use of the passive techniques has proven effectiveness to improve the thermal performance in a microchannel. However, the using of single technique such as corrugated MCHS, ribs, cavities and interrupted wall channels have shown two trends of enhancement; either high heat transfer rate associated with high pressure drop or low rate of heat transfer associated with low pressure drop. So, until now, it is difficult to find the best compromise value for both heat transfer and pressure drop. Besides, the using of single configuration has reached to the ultimate enhancement status and there is a need for more enhancement to keep pace with rapidly growing toward the higher performance electronic.

The current research attempts to propose of using two passive technique to enhance heat transfer in MCHS rather than using single technique. This strategy aimed to reduce the high pressure drop by increasing the flow area and at the same time increase heat transfer rate through increasing heat transfer area, flow mixing, promote jet impingement and Dean vortices.

1.5 Objectives of the work

The aim of the present work is to develop and analyze the effect of the combination between two passive techniques in three new designs of microchannel heat sink in order to assess a potential interaction between both techniques for further heat transfer enhancement.

This study sets the following objectives.

1. The first objective is to analyze numerically the hydrothermal characteristics of the proposed designs to explore the effectiveness of combination between passive techniques on the thermal performance. Three models are proposed to be analyzed. The first model is combining between wavy microchannel with oblique secondary channels. The second model is utilizing the sinusoidal cavities arranged on the side walls of microchannel with ribs in the central portion of the channel. The third model is merging between oblique secondary channels and ribs.
2. To optimize the geometrical parameters of the proposed models in order to achieve the desired values for both pressure drop and heat transfer characteristics that attain maximum overall performance.
3. The third objective is to validate the numerical results for the first model experimentally by using a full-scale microchannel heat sink experimental rig. The validation of the CFD results aims to analyze the deviation between observed and simulated results in order to examine the ability of numerical simulation to predict the characteristics of fluid flow and heat transfer in proposed design.

1.6 Scope

The recurring theme of the present thesis is to enhance heat transfer in microchannel heat sink using hybrid techniques of passive heat transfer methods. The study is concentrated on using two methods; flow disruption and corrugated channel in three new configurations. The techniques that have been followed are the integration of wavy channel with secondary channel, ribs with cavities and ribs with secondary channels. Based on the objectives, the following scopes are defined:

1. To study the hydrothermal characteristics of the proposed designs, numerical simulations have been conducted using three-dimensional CFD models consist of one row channel. The geometries are modelled and simulated using ANSYS workbench CFD software version 14. The numerical simulation is covered both laminar and turbulent flow regime. The variation of two parameters are considered, namely heat flux and velocity of inlet water. The range of heat flux is between 50-100W/cm² and Reynolds number ranged between 100-1200. The SIMPLE algorithm was adopted to accomplish the pressure-velocity coupling. At the same time, the second order upwind scheme is used for convective term and second order central difference scheme is applied for diffusion term. K-epsilon model has been used to solve turbulent flow. For all proposed models, constant inlet velocity and constant heat flux are the adopted as a boundary conditions in simulation
2. In this study, an experimental setup comprising of heating system, water distribution system and measurement instrumentation is developed to resemble the cooling system of electronic devices. Microchannel heat sink with wavy channels and oblique secondary channels (WMSC) is tested on this rig. The heat sinks device consisting of 31 microchannels arranged in multiple rows with ten waves in each single row. Each microchannel has a dimensions of 20 mm length, 200 μm width and 400 μm height and structured on a surface area of 2.8 cm². The heat flux at the heating surface is varied between 50 W/cm² to 100 W/cm², while the flow rate is varied between 112ml/min until 448.5 ml/min

1.7 Chapter summary

This chapter described the concept of heat transfer enhancement techniques in general and clarifying the applicability in microchannel heat sink. This is meant to relate the current problem of restrictions that hinder the heat transfer enhancement in microchannel heat sink with purpose of this study. Besides, the problem statement, objectives and scope of work have been presented in detail.

REFERENCES

- [1] Y. J. Lee, P. K. Singh, and P. S. Lee, "Fluid flow and heat transfer investigations on enhanced microchannel heat sink using oblique fins with parametric study," *International Journal of Heat and Mass Transfer*, vol. 81, pp. 325-336, 2015.
- [2] H. Ghaedamini, P. S. Lee, and C. J. Teo, "Developing forced convection in converging–diverging microchannels," *International Journal of Heat and Mass Transfer*, vol. 65, pp. 491-499, 2013.
- [3] C. Moore, "Data processing in exascale-class computer systems," in *The Salishan Conference on High Speed Computing*, 2011.
- [4] S. G. Kandlikar and W. J. Grande, "Evaluation of Single Phase Flow in Microchannels for High Heat Flux Chip Cooling—Thermohydraulic Performance Enhancement and Fabrication Technology," *Heat Transfer Engineering*, vol. 25, pp. 5-16, 2004.
- [5] D. B. Tuckerman and R. Pease, "High-performance heat sinking for VLSI," *Electron Device Letters, IEEE*, vol. 2, pp. 126-129, 1981.
- [6] Y. Sui, C. J. Teo, P. S. Lee, Y. T. Chew, and C. Shu, "Fluid flow and heat transfer in wavy microchannels," *International Journal of Heat and Mass Transfer*, vol. 53, pp. 2760-2772, 2010.
- [7] X. Peng and G. Peterson, "Convective heat transfer and flow friction for water flow in microchannel structures," *International journal of heat and mass transfer*, vol. 39, pp. 2599-2608, 1996.
- [8] M. M. Rahman and F. Gui, "Experimental measurements of fluid flow and heat transfer in microchannel cooling passages in a chip substrate," in *The ASME International Electronics Packaging Conference, Binghamton, NY, USA*, 1993, pp. 685-692.

- [9] G. Gamrat, M. Favre-Marinet, and D. Asendrych, "Conduction and entrance effects on laminar liquid flow and heat transfer in rectangular microchannels," *International Journal of Heat and Mass Transfer*, vol. 48, pp. 2943-2954, 2005.
- [10] T. M. Harms, M. J. Kazmierczak, and F. M. Gerner, "Developing convective heat transfer in deep rectangular microchannels," *International Journal of Heat and Fluid Flow*, vol. 20, pp. 149-157, 1999.
- [11] W. Owhaib and B. Palm, "Experimental investigation of single-phase convective heat transfer in circular microchannels," *Experimental Thermal and Fluid Science*, vol. 28, pp. 105-110, 2004.
- [12] J. P. McHale and S. V. Garimella, "Heat transfer in trapezoidal microchannels of various aspect ratios," *International Journal of Heat and Mass Transfer*, vol. 53, pp. 365-375, 2010.
- [13] Y. Chen, C. Zhang, M. Shi, and J. Wu, "Three-dimensional numerical simulation of heat and fluid flow in noncircular microchannel heat sinks," *International Communications in Heat and Mass Transfer*, vol. 36, pp. 917-920, 2009.
- [14] A. Tamayol and M. Bahrami, "Laminar flow in microchannels with noncircular cross section," *Journal of Fluids Engineering*, vol. 132, p. 111201, 2010.
- [15] H. Mohammed, P. Gunnasegaran, and N. Shuaib, "The impact of various nanofluid types on triangular microchannels heat sink cooling performance," *International Communications in Heat and Mass Transfer*, vol. 38, pp. 767-773, 2011.
- [16] A. Agarwal, T. M. Bandhauer, and S. Garimella, "Measurement and modeling of condensation heat transfer in non-circular microchannels," *international journal of refrigeration*, vol. 33, pp. 1169-1179, 2010.
- [17] P.-S. Lee, S. V. Garimella, and D. Liu, "Investigation of heat transfer in rectangular microchannels," *International Journal of Heat and Mass Transfer*, vol. 48, pp. 1688-1704, 2005.
- [18] P. Gunnasegaran, H. Mohammed, N. Shuaib, and R. Saidur, "The effect of geometrical parameters on heat transfer characteristics of microchannels heat

- sink with different shapes," *International Communications in Heat and Mass Transfer*, vol. 37, pp. 1078-1086, 2010.
- [19] W. Q. Tao, Y. L. He, Q. W. Wang, Z. G. Qu, and F. Q. Song, "A unified analysis on enhancing single phase convective heat transfer with field synergy principle," *International Journal of Heat and Mass Transfer*, vol. 45, pp. 4871-4879, 2002.
- [20] M. E. Steinke and S. G. Kandlikar, "Review of single-phase heat transfer enhancement techniques for application in microchannels, minichannels and microdevices," *International Journal of Heat and Technology*, vol. 22, pp. 3-11, 2004.
- [21] A. E. Bergles, "ExHFT for fourth generation heat transfer technology," *Experimental Thermal and Fluid Science*, vol. 26, pp. 335-344, 2002.
- [22] A. E. Bergles, "Heat transfer enhancement - The encouragement and accommodation of high heat fluxes," *Journal of Heat Transfer*, vol. 119, pp. 8-19, 1997.
- [23] A. E. Bergles, "Enhanced heat transfer: Endless frontier, or mature and routine?," *Journal of Enhanced Heat Transfer*, vol. 6, pp. 79-88, 1999.
- [24] A. Dewan, P. Mahanta, K. S. Raju, and P. S. Kumar, "Review of passive heat transfer augmentation techniques," *Proceedings of the Institution of Mechanical Engineers, Part A: Journal of Power and Energy*, vol. 218, pp. 509-527, 2004.
- [25] L. Leal, M. Miscevic, P. Lavieille, M. Amokrane, F. Pigache, F. Topin, *et al.*, "An overview of heat transfer enhancement methods and new perspectives: Focus on active methods using electroactive materials," *International Journal of Heat and Mass Transfer*, vol. 61, pp. 505-524, 2013.
- [26] J. F. Tullius, R. Vajtai, and Y. Bayazitoglu, "A Review of Cooling in Microchannels," *Heat Transfer Engineering*, vol. 32, pp. 527-541, 2011.
- [27] A. Dewan and P. Srivastava, "A review of heat transfer enhancement through flow disruption in a microchannel," *Journal of Thermal Science*, vol. 24, pp. 203-214, 2015.
- [28] L. Wang and T. Yang, "Bifurcation and stability of forced convection in curved ducts of square cross-section," *International Journal of Heat and Mass Transfer*, vol. 47, pp. 2971-2987, 2004.

- [29] W. R. Dean, "XVI. Note on the motion of fluid in a curved pipe," *The London, Edinburgh, and Dublin Philosophical Magazine and Journal of Science*, vol. 4, pp. 208-223, 1927.
- [30] W. R. Dean, "LXXII. The stream-line motion of fluid in a curved pipe (Second paper)," *The London, Edinburgh, and Dublin Philosophical Magazine and Journal of Science*, vol. 5, pp. 673-695, 1928.
- [31] A. Mokrani, C. Castelain, and H. Peerhossaini, "The effects of chaotic advection on heat transfer," *International Journal of Heat and Mass Transfer*, vol. 40, pp. 3089-3104, 1997.
- [32] S. Sugiyama, T. Hayashi, and K. Yamazaki, "Flow Characteristics in the Curved Rectangular Channels: Visualization of Secondary Flow," *Bulletin of JSME*, vol. 26, pp. 964-969, 1983.
- [33] C. Kalb and J. Seader, "Heat and mass transfer phenomena for viscous flow in curved circular tubes," *International Journal of Heat and Mass Transfer*, vol. 15, pp. 801-817, 1972.
- [34] J. H. Masliyah and K. Nandakumar, "Fully developed viscous flow and heat transfer in curved semicircular sectors," *AIChE Journal*, vol. 25, pp. 478-487, 1979.
- [35] K. Cheng, R.-C. Lin, and J.-W. Ou, "Fully developed laminar flow in curved rectangular channels," *Journal of Fluids Engineering*, vol. 98, pp. 41-48, 1976.
- [36] N. R. Rosaguti, D. F. Fletcher, and B. S. Haynes, "Laminar flow and heat transfer in a periodic serpentine channel," *Chemical engineering & technology*, vol. 28, pp. 353-361, 2005.
- [37] N. R. Rosaguti, D. F. Fletcher, and B. S. Haynes, "Laminar flow and heat transfer in a periodic serpentine channel with semi-circular cross-section," *International journal of heat and mass transfer*, vol. 49, pp. 2912-2923, 2006.
- [38] P. E. Geyer, N. R. Rosaguti, D. F. Fletcher, and B. S. Haynes, "Thermohydraulics of square-section microchannels following a serpentine path," *Microfluidics and Nanofluidics*, vol. 2, pp. 195-204, 2005.
- [39] P. E. Geyer, N. R. Rosaguti, D. F. Fletcher, and B. S. Haynes, "Laminar flow and heat transfer in periodic serpentine mini-channels," *Journal of Enhanced Heat Transfer*, vol. 13, 2006.

- [40] P. E. Geyer, D. F. Fletcher, and B. S. Haynes, "Laminar flow and heat transfer in a periodic trapezoidal channel with semi-circular cross-section," *International journal of heat and mass transfer*, vol. 50, pp. 3471-3480, 2007.
- [41] H. Metwally and R. M. Manglik, "Enhanced heat transfer due to curvature-induced lateral vortices in laminar flows in sinusoidal corrugated-plate channels," *International Journal of Heat and Mass Transfer*, vol. 47, pp. 2283-2292, 2004.
- [42] R. M. Manglik, J. Zhang, and A. Muley, "Low Reynolds number forced convection in three-dimensional wavy-plate-fin compact channels: fin density effects," *International Journal of Heat and Mass Transfer*, vol. 48, pp. 1439-1449, 2005.
- [43] C. Chagny, C. Castelain, and H. Peerhossaini, "Chaotic heat transfer for heat exchanger design and comparison with a regular regime for a large range of Reynolds numbers," *Applied Thermal Engineering*, vol. 20, pp. 1615-1648, 2000.
- [44] Z. Zheng, D. F. Fletcher, and B. S. Haynes, "Laminar heat transfer simulations for periodic zigzag semicircular channels: chaotic advection and geometric effects," *International Journal of Heat and Mass Transfer*, vol. 62, pp. 391-401, 2013.
- [45] R. H. Liu, M. A. Stremler, K. V. Sharp, M. G. Olsen, J. G. Santiago, R. J. Adrian, *et al.*, "Passive mixing in a three-dimensional serpentine microchannel," *Journal of Microelectromechanical Systems*, vol. 9, pp. 190-197, 2000.
- [46] H. Aref, "Stirring by chaotic advection," *Journal of fluid mechanics*, vol. 143, pp. 1-21, 1984.
- [47] H. Peerhossaini, C. Castelain, and Y. Le Guer, "Heat exchanger design based on chaotic advection," *Experimental thermal and fluid science*, vol. 7, pp. 333-344, 1993.
- [48] Y. Sui, P. S. Lee, and C. J. Teo, "An experimental study of flow friction and heat transfer in wavy microchannels with rectangular cross section," *International Journal of Thermal Sciences*, vol. 50, pp. 2473-2482, 2011.

- [49] Y. Sui, C. Teo, and P. Lee, "Direct numerical simulation of fluid flow and heat transfer in periodic wavy channels with rectangular cross-sections," *International Journal of Heat and Mass Transfer*, vol. 55, pp. 73-88, 2012.
- [50] H. Mohammed, P. Gunnasegaran, and N. Shuaib, "Numerical simulation of heat transfer enhancement in wavy microchannel heat sink," *International Communications in Heat and Mass Transfer*, vol. 38, pp. 63-68, 2011.
- [51] G. Xie, J. Liu, Y. Liu, B. Sunden, and W. Zhang, "Comparative study of thermal performance of longitudinal and transversal-wavy microchannel heat sinks for electronic cooling," *Journal of Electronic Packaging*, vol. 135, pp. 1-9, 2013.
- [52] G. Xie, J. Liu, W. Zhang, and B. Sunden, "Analysis of flow and thermal performance of a water-cooled transversal wavy microchannel heat sink for chip cooling," *Journal of Electronic Packaging*, vol. 134, pp. 1-11, 2012.
- [53] W. M. Abed, R. D. Whalley, D. J. C. Dennis, and R. J. Poole, "Numerical and experimental investigation of heat transfer and fluid flow characteristics in a micro-scale serpentine channel," *International Journal of Heat and Mass Transfer*, vol. 88, pp. 790-802, 2015.
- [54] L. Gong, K. Kota, W. Tao, and Y. Joshi, "Parametric numerical study of flow and heat transfer in microchannels with wavy walls," *Journal of Heat Transfer*, vol. 133, pp. 1-13, 2011.
- [55] J. Yong and C. J. Teo, "Mixing and heat transfer enhancement in microchannels containing converging-diverging passages," *Journal of Heat Transfer*, vol. 136, p. 041704, 2014.
- [56] H. Mohammed, P. Gunnasegaran, and N. Shuaib, "Influence of channel shape on the thermal and hydraulic performance of microchannel heat sink," *International Communications in Heat and Mass Transfer*, vol. 38, pp. 474-480, 2011.
- [57] Z. Dai, Z. Zheng, D. F. Fletcher, and B. S. Haynes, "Experimental study of transient behaviour of laminar flow in zigzag semi-circular microchannels," *Experimental Thermal and Fluid Science*, vol. 68, pp. 644-651, 2015.
- [58] Z. Dai, D. F. Fletcher, and B. S. Haynes, "Impact of tortuous geometry on laminar flow heat transfer in microchannels," *International Journal of Heat and Mass Transfer*, vol. 83, pp. 382-398, 2015.

- [59] C. Amon, D. Majumdar, C. Herman, F. Mayinger, B. Mikic, and D. Sekulic, "Numerical and experimental studies of self-sustained oscillatory flows in communicating channels," *International Journal of Heat and Mass Transfer*, vol. 35, pp. 3115-3129, 1992.
- [60] N. Ghaddar, K. Korczak, B. Mikic, and A. Patera, "Numerical investigation of incompressible flow in grooved channels. Part 1. Stability and self-sustained oscillations," *Journal of Fluid Mechanics*, vol. 163, pp. 99-127, 1986.
- [61] N. Ghaddar, M. Magen, B. Mikic, and A. Patera, "Numerical investigation of incompressible flow in grooved channels. Part 2. Resonance and oscillatory heat-transfer enhancement," *Journal of Fluid Mechanics*, vol. 168, pp. 541-567, 1986.
- [62] M. Greiner, R.-F. Chen, and R. Wirtz, "Enhanced heat transfer/pressure drop measured from a flat surface in a grooved channel," *Journal of heat transfer*, vol. 113, pp. 498-501, 1991.
- [63] R. Wirtz, F. Huang, and M. Greiner, "Correlation of fully developed heat transfer and pressure drop in a symmetrically grooved channel," *Journal of heat transfer*, vol. 113, pp. 590-596, 1999.
- [64] C. Herman and E. Kang, "Experimental visualization of temperature fields and study of heat transfer enhancement in oscillatory flow in a grooved channel," *Heat and Mass Transfer*, vol. 37, pp. 87-99, 2001.
- [65] S. Lorenz, D. Mukomilow, and W. Leiner, "Distribution of the heat transfer coefficient in a channel with periodic transverse grooves," *Experimental Thermal and Fluid Science*, vol. 11, pp. 234-242, 1995.
- [66] C. Herman and F. Mayinger, "Experimental analysis of forced convection heat transfer in a grooved channel," *Adv. Heat Transfer*, pp. 900-913, 1992.
- [67] L. Wang and B. Sundén, "Experimental investigation of local heat transfer in a square duct with various-shaped ribs," *Heat and Mass Transfer*, vol. 43, pp. 759-766, 2007.
- [68] C. Herman and E. Kang, "Heat transfer enhancement in a grooved channel with curved vanes," *International Journal of Heat and Mass Transfer*, vol. 45, pp. 3741-3757, 2002.

- [69] Y. Islamoglu and C. Parmaksizoglu, "The effect of channel height on the enhanced heat transfer characteristics in a corrugated heat exchanger channel," *Applied Thermal Engineering*, vol. 23, pp. 979-987, 2003.
- [70] E. A. M. Elshafei, M. M. Awad, E. El-Negiry, and A. G. Ali, "Heat transfer and pressure drop in corrugated channels," *Energy*, vol. 35, pp. 101-110, 2010.
- [71] A. Hartmann and A. Lucic, "Application of the holographic interferometry in transport phenomena studies," *Heat and mass transfer*, vol. 37, pp. 549-562, 2001.
- [72] J. Cernecky, J. Koniar, and Z. Brodnianska, "The Effect of Heat Transfer Area Roughness on Heat Transfer Enhancement by Forced Convection," *Journal of Heat Transfer*, vol. 136, p. 041901, 2014.
- [73] G. Xia, L. Chai, M. Zhou, and H. Wang, "Effects of structural parameters on fluid flow and heat transfer in a microchannel with aligned fan-shaped reentrant cavities," *International Journal of Thermal Sciences*, vol. 50, pp. 411-419, 2011.
- [74] L. Chai, G. Xia, M. Zhou, and J. Li, "Numerical simulation of fluid flow and heat transfer in a microchannel heat sink with offset fan-shaped reentrant cavities in sidewall," *International Communications in Heat and Mass Transfer*, vol. 38, pp. 577-584, 2011.
- [75] G. Xia, L. Chai, H. Wang, M. Zhou, and Z. Cui, "Optimum thermal design of microchannel heat sink with triangular reentrant cavities," *Applied Thermal Engineering*, vol. 31, pp. 1208-1219, 2011.
- [76] L. Chai, G. Xia, L. Wang, M. Zhou, and Z. Cui, "Heat transfer enhancement in microchannel heat sinks with periodic expansion–constriction cross-sections," *International Journal of Heat and Mass Transfer*, vol. 62, pp. 741-751, 2013.
- [77] G. D. Xia, J. Jiang, J. Wang, Y. L. Zhai, and D. D. Ma, "Effects of different geometric structures on fluid flow and heat transfer performance in microchannel heat sinks," *International Journal of Heat and Mass Transfer*, vol. 80, pp. 439-447, 2015.
- [78] G. Xia, D. Ma, Y. Zhai, Y. Li, R. Liu, and M. Du, "Experimental and numerical study of fluid flow and heat transfer characteristics in microchannel heat sink with complex structure," *Energy Conversion and Management*, vol. 105, pp. 848-857, 2015.

- [79] O. Abouali and N. Baghernezhad, "Numerical investigation of heat transfer enhancement in a microchannel with grooved surfaces," *Journal of Heat Transfer*, vol. 132, pp. 1-10, 2010.
- [80] D. Ansari, A. Husain, and K.-Y. Kim, "Multiobjective optimization of a grooved micro-channel heat sink," *Components and Packaging Technologies, IEEE Transactions on*, vol. 33, pp. 767-776, 2010.
- [81] N. R. Kuppusamy, H. A. Mohammed, and C. W. Lim, "Numerical investigation of trapezoidal grooved microchannel heat sink using nanofluids," *Thermochimica Acta*, vol. 573, pp. 39-56, 2013.
- [82] N. R. Kuppusamy, H. A. Mohammed, and C. W. Lim, "Thermal and hydraulic characteristics of nanofluid in a triangular grooved microchannel heat sink (TGMCHS)," *Applied Mathematics and Computation*, vol. 246, pp. 168-183, 2014.
- [83] H. E. Ahmed and M. I. Ahmed, "Optimum thermal design of triangular, trapezoidal and rectangular grooved microchannel heat sinks," *International Communications in Heat and Mass Transfer*, vol. 66, pp. 47-57, 2015.
- [84] L. Chai, G. D. Xia, and H. S. Wang, "Parametric study on thermal and hydraulic characteristics of laminar flow in microchannel heat sink with fan-shaped ribs on sidewalls – Part 1: Heat transfer," *International Journal of Heat and Mass Transfer*, vol. 97, pp. 1069-1080, 2016.
- [85] L. Chai, G. D. Xia, and H. S. Wang, "Parametric study on thermal and hydraulic characteristics of laminar flow in microchannel heat sink with fan-shaped ribs on sidewalls – Part 2: Pressure drop," *International Journal of Heat and Mass Transfer*, vol. 97, pp. 1081-1090, 2016.
- [86] L. Chai, G. D. Xia, and H. S. Wang, "Parametric study on thermal and hydraulic characteristics of laminar flow in microchannel heat sink with fan-shaped ribs on sidewalls – Part 3: Performance evaluation," *International Journal of Heat and Mass Transfer*, vol. 97, pp. 1091-1101, 2016.
- [87] L. Chai, G. D. Xia, and H. S. Wang, "Numerical study of laminar flow and heat transfer in microchannel heat sink with offset ribs on sidewalls," *Applied Thermal Engineering*, vol. 92, pp. 32-41, 2016.

- [88] G. Xia, Y. Zhai, and Z. Cui, "Numerical investigation of thermal enhancement in a micro heat sink with fan-shaped reentrant cavities and internal ribs," *Applied Thermal Engineering*, vol. 58, pp. 52-60, 2013.
- [89] Y. L. Zhai, G. D. Xia, X. F. Liu, and Y. F. Li, "Heat transfer in the microchannels with fan-shaped reentrant cavities and different ribs based on field synergy principle and entropy generation analysis," *International Journal of Heat and Mass Transfer*, vol. 68, pp. 224-233, 2014.
- [90] Y. Zhai, G. Xia, X. Liu, and Y. Li, "Exergy analysis and performance evaluation of flow and heat transfer in different micro heat sinks with complex structure," *International Journal of Heat and Mass Transfer*, vol. 84, pp. 293-303, 2015.
- [91] Y. Xie, Z. Shen, D. Zhang, and J. Lan, "Thermal performance of a water-cooled microchannel heat sink with grooves and obstacles," *Journal of Electronic Packaging*, vol. 136, pp. 1-13, 2014.
- [92] G. Wang, D. Niu, F. Xie, Y. Wang, X. Zhao, and G. Ding, "Experimental and numerical investigation of a microchannel heat sink (MCHS) with micro-scale ribs and grooves for chip cooling," *Applied Thermal Engineering*, vol. 85, pp. 61-70, 2015.
- [93] Y. Li, G. Xia, D. Ma, Y. Jia, and J. Wang, "Characteristics of laminar flow and heat transfer in microchannel heat sink with triangular cavities and rectangular ribs," *International Journal of Heat and Mass Transfer*, vol. 98, pp. 17-28, 2016.
- [94] M. E. Steinke and S. G. Kandlikar, "Single-phase liquid heat transfer in plain and enhanced microchannels," in *ASME 4th International Conference on Nanochannels, Microchannels, and Minichannels*, 2006, pp. 943-951.
- [95] T. Kishimoto and S. Sasaki, "Cooling characteristics of diamond-shaped interrupted cooling fin for high-power LSI devices," *Electronics Letters*, vol. 23, pp. 456-457, 1987.
- [96] S. G. Kandlikar and H. R. Upadhye, "Extending the heat flux limit with enhanced microchannels in direct single-phase cooling of computer chips," in *Semiconductor Thermal Measurement and Management Symposium, 2005 IEEE Twenty First Annual IEEE*, 2005, pp. 8-15.

- [97] E. G. Colgan, B. Furman, M. Gaynes, W. S. Graham, N. C. LaBianca, J. H. Magerlein, *et al.*, "A practical implementation of silicon microchannel coolers for high power chips," *Components and Packaging Technologies, IEEE Transactions on*, vol. 30, pp. 218-225, 2007.
- [98] F. Hong and P. Cheng, "Three dimensional numerical analyses and optimization of offset strip-fin microchannel heat sinks," *International Communications in Heat and Mass Transfer*, vol. 36, pp. 651-656, 2009.
- [99] E. Sparrow, B. Baliga, and S. Patankar, "Heat transfer and fluid flow analysis of interrupted-wall channels, with application to heat exchangers," *Journal of Heat Transfer*, vol. 99, pp. 4-11, 1977.
- [100] J. L. Xu, Y. H. Gan, D. C. Zhang, and X. H. Li, "Microscale heat transfer enhancement using thermal boundary layer redeveloping concept," *International Journal of Heat and Mass Transfer*, vol. 48, pp. 1662-1674, 2005.
- [101] J. Xu, Y. Song, W. Zhang, H. Zhang, and Y. Gan, "Numerical simulations of interrupted and conventional microchannel heat sinks," *International Journal of Heat and Mass Transfer*, vol. 51, pp. 5906-5917, 2008.
- [102] L. Chai, G. Xia, M. Zhou, J. Li, and J. Qi, "Optimum thermal design of interrupted microchannel heat sink with rectangular ribs in the transverse microchambers," *Applied Thermal Engineering*, vol. 51, pp. 880-889, 2013.
- [103] Y.-J. Lee, P.-S. Lee, and S.-K. Chou, "Enhanced microchannel heat sinks using oblique fins," in *ASME 2009 InterPACK Conference collocated with the ASME 2009 Summer Heat Transfer Conference and the ASME 2009 3rd International Conference on Energy Sustainability*, 2009, pp. 253-260.
- [104] K. Suga and H. Aoki, "Numerical Study on Heat Transfer and Pressure Drop in Multilouvered Fins," vol. 2, pp. 231-238, 1995.
- [105] N. C. DeJong and A. M. Jacobi, "Localized flow and heat transfer interactions in louvered-fin arrays," *International Journal of Heat and Mass Transfer*, vol. 46, pp. 443-455, 2003.
- [106] Y.-J. Lee, P.-S. Lee, and S.-K. Chou, "Experimental investigation of oblique finned microchannel heat sink+," in *Thermal and Thermomechanical Phenomena in Electronic Systems (ITherm), 2010 12th IEEE Intersociety Conference on*, 2010, pp. 1-7.

- [107] Y.-J. Lee, P.-S. Lee, and S.-K. Chou, "Experimental Investigation of Silicon-Based Oblique Finned Microchannel Heat Sinks," in *2010 14th International Heat Transfer Conference*, 2010, pp. 283-291.
- [108] Y. Lee, P. Lee, and S. Chou, "Enhanced thermal transport in microchannel using oblique fins," *Journal of Heat Transfer*, vol. 134, p. 101901, 2012.
- [109] N. R. Kuppusamy, R. Saidur, N. Ghazali, and H. Mohammed, "Numerical study of thermal enhancement in micro channel heat sink with secondary flow," *International Journal of Heat and Mass Transfer*, vol. 78, pp. 216-223, 2014.
- [110] R. F. Service, "Coming Soon: The Pocket DNA Sequencer," *Science*, vol. 282, pp. 399-401, 1998.
- [111] W. Qu, "Transport phenomena in single-phase and two-phase micro-channel heat sinks," 2004.
- [112] N. E. Todreas and M. S. Kazimi, *Nuclear systems: thermal hydraulic fundamentals* vol. 1: CRC press, 2012.
- [113] W. M. Kays and A. L. London, "Compact heat exchangers," 1984.
- [114] J. M. Ottino, *The kinematics of mixing: stretching, chaos, and transport* vol. 3: Cambridge university press, 1989.
- [115] F. Schönfeld and S. Hardt, "Simulation of helical flows in microchannels," *AIChE Journal*, vol. 50, pp. 771-778, 2004.
- [116] F. Jiang, K. Drese, S. Hardt, M. Küpper, and F. Schönfeld, "Helical flows and chaotic mixing in curved micro channels," *AIChE journal*, vol. 50, pp. 2297-2305, 2004.
- [117] H. W. Coleman and W. G. Steele, *Experimentation, validation, and uncertainty analysis for engineers*: John Wiley & Sons, 2009.
- [118] M. E. Steinke and S. G. Kandlikar, "Single-phase liquid friction factors in microchannels," *International Journal of Thermal Sciences*, vol. 45, pp. 1073-1083, 2006.
- [119] R. J. Phillips, "Microchannel heat sinks," *Advances in thermal modeling of electronic components and systems*, vol. 2, pp. 109-184, 1990.
- [120] R. L. Webb, "Performance evaluation criteria for use of enhanced heat transfer surfaces in heat exchanger design," *International Journal of Heat and Mass Transfer*, vol. 24, pp. 715-726, 1981.

- [121] J. H. Kim, T. W. Simon, and R. Viskanta, "Journal of heat transfer policy on reporting uncertainties in experimental measurements and results," *Journal of Heat Transfer*, vol. 115, pp. 5-6, 1993.